Tumor angiogenesis mediated by myeloid cells is negatively regulated by CEACAM-1

Rongze Lu[1,2,3], **Maciej Kujawski**[2], **Hao Pan**[1,2,4], and **John E. Shively**[2]

[1]City of Hope Irell & Manella Graduate School of Biological Sciences, Duarte, CA 91010

[2]Department of Immunology, Beckman Research Institute of City of Hope, 1450 E. Duarte Rd, Duarte CA 91010, USA

Abstract

Bv8 (prokineticin 2) expressed by $Gr1^+CD11b^+$ myeloid cells is critical for VEGF-independent tumor angiogenesis. Although G-CSF has been shown to be a key inducer of Bv8 expression, the basis for Bv8 production in driving tumor angiogenesis is undefined. Since the cell adhesion molecule CEACAM1 that is highly expressed on Gr1+CD11b+ myeloid cells is known to regulate G-CSFR signaling, we hypothesized that CEACAM1 would regulate Bv8 production in these cells. In support of this hypothesis we found that Bv8 expression was elevated in $Gr1^+CD11b^+$ cells from Ceacam1-deficient mice implanted with B16 melanoma, increasing the infiltration of $Gr1^+CD11b^+$ myeloid cells in melanoma tumors and enhancing their growth and angiogenesis. Further, treatment with anti-Gr1 or anti-Bv8 or anti-G-CSF monoclonal antibody reduced myeloid cell infiltration, tumor growth, and angiogenesis to levels observed in tumor bearing wild-type mice. Reconstitution of CEACAM1-deficient mice with wild type bone marrow cells restored tumor infiltration of Gr1+CD11b+ cells along with tumor growth and angiogenesis. Treatment of tumor bearing wild-type mice with anti-CEACAM1 antibody limited tumor outgrowth and angiogenesis, albeit to a lesser extent. Tumor growth in Ceacam1-deficient mice was not affected significantly in $Rag^{-/-}$ background, indicating that CEACAM1 expression in T- and B-lymphocytes had a negligible role in this pathway. Together, our findings demonstrate that CEACAM1 negatively regulates $Gr1^+CD11b^+$ myeloid cell dependent tumor angiogenesis by inhibiting the G-CSF-Bv8 signaling pathway.

Keywords

CEACAM1: Carcinoembryonic antigen-related cell adhesion molecule 1; Myeloid cells; angiogenesis; Bv8: Bombina variagata peptide 8; G-CSF: Granulocyte colony-stimulating factor

Introduction

Since tumor growth is strictly dependent on angiogenesis, the identification of tumor angiogenic factors and the cells that produce them is a major goal. Although VEGF was identified as one of the most potent angiogenic factors, many tumors become resistant to anti-VEGF therapy (1). Myeloid cells that express surface markers Gr1 and CD11b are the main regulators of tumor refractoriness to anti-VEGF treatment in immunocompetent rodent tumor models (1). $Gr1^+CD11b^+$ cells promote resistance to anti-VEGF therapy by

Correspondence should be addressed to: J.E. Shively, JShively@coh.org.
[3]Current address: Genentech, Inc, South San Francisco CA
[4]Current address: Nexcelom Bioscience, Lawrence, MA 01843

There are no conflicts of interest.

expression of matrix metallopeptidase 9 (MMP9) or by direct incorporation into the endothelium (2). Among the signaling pathways studied, Stat3 is a key signal transducer in $Gr1^+CD11b^+$ cell-mediated tumor angiogenesis (3). More recently, the pro-angiogenic factor Bv8 or prokineticin2 has been shown to be specifically upregulated by G-CSF in anti-VEGF refractory tumors (4, 5). The pro-angiogenic activities of $Gr1^+CD11b^+$ cells depend on G-CSF, starting from the bone marrow and continuing with their migration to the tumor, promoting both angiogenesis and tumor invasion (6–8). Thus, regulation of Bv8 production by $Gr1^+CD11b^+$ myeloid cells is a new target for the inhibition of tumor growth and angiogenesis (5, 9, 10).

Bv8 was first characterized as a protein of 77 amino acids from bombina variegata skin secretions, and later shown to have 70% similarity to endocrine gland-derived vascular endothelial growth factor (EG-VEGF) or prokineticins-1 and −2 (8, 11). Both have a five-disulfide-bridge motif and associate with G-protein coupled receptors, EG-VEGFR1 (or PKR1) and EG-VEGFR2 (or PKR2) (8, 11). Bv8 promotes proliferation of endothelial cells, hematopoiesis and hematopoietic cell migration (8, 12). Blocking Bv8 or its upregulator G-CSF in tumor bearing mice with either anti-Bv8 or anti-G-CSF neutralizing antibodies inhibits tumor angiogenesis and tumor growth (5, 7). However, the mechanism of G-CSF regulation of Bv8 in Gr1+ CD11b+ cells has not been studied. Thus, identification of negative regulators of these cells presents an opportunity to control their pro-tumorigenic activities.

We have recently identified Carcinoembryonic Antigen-related Cell Adhesion Moclecule-1 (CEACAM1) as a critical regulator of granulopoiesis which depends on G-CSF-R and Stat3 signaling (13). CEACAM1, highly expressed on granulocytes in both man and rodents, has multiple splice forms including a long cytoplasmic domain isoform that encodes two ITIMs (14). Phosphorylation of its ITIMs recruits the inhibitory phosphatase SHP-1, that in turn, dephosphorylates G-CSFR, thus inhibiting the pro-granulocytic activity of G-CSFR (13). Although CEACAM1 is recognized as a tumor suppressor gene due to its down-regulation in solid tumors including colon (15), prostate (16) and breast (17), the mechanism is not well understood. In fact, in some tumors such as melanoma, up-regulation of CEACAM1 has been observed, throwing doubt on its role as a general tumor suppressor (18, 19). Although tumor growth in Ceacam1$^{-/-}$ mice is accelerated (20, 21), the role of CEACAM1 expression in the tumor is controversial. Alternatively, the function of CEACAM1 in myeloid cells and lymphocytes may play a larger role than the expression of CEACAM1 itself in tumors. In this respect, we are interested in connecting the very high expression of CEACAM1 in $Gr1^+CD11b^+$ cells and its role in G-CSF signaling to its newly assigned role in angiogenesis. For example, Ergun and coworkers have shown that CEACAM1 plays a significant role in angiogenesis in endothelial cells (22–25) and we have shown that CEACAM1 is required for vasculogenesis in embryonic stem cells (26). In spite of these connections, the mechanism of CEACAM1's function in myeloid-cell mediated tumor angiogenesis is unknown.

In this study, we demonstrate that genetic loss of CEACAM1 leads to increased Bv8 expression in $Gr1^+CD11b^+$ cells, as well as enhanced tumor growth and angiogenesis. Reconstitution of CEACAM1$^{-/-}$ mice with wild type bone marrow cells restored infiltration of Gr1+CD11b+ cells, as well as tumor growth and angiogenesis to wild type levels. Blocking Bv8 or G-CSF in CEACAM1$^{-/-}$ tumor bearing mice with monoclonal antibodies reduced tumor infiltration of $Gr1^+CD11b^+$ myeloid cells, with accompanied enhanced tumor growth and angiogenesis to levels observed in untreated controls. Anti-CEACAM1 antibody treatment decreased $Gr1^+CD11b^+$ myeloid cell infiltration into the blood and spleen, which in turn reduced tumor angiogenesis and tumor growth in wild type mice. These results

underscore the inhibitory role of CEACAM1 in myeloid cell mediated tumor angiogenesis, indicating that CEACAM1 is a promising target for tumor immunotherapy.

Material and Methods

Antibodies

Anti-Bv8 antibodies 2B9 and 3F1 were from Genentech, Inc. (South San Francisco, CA), anti-G-CSF MAB414 and isotype control from R&D Systems (Minneapolis, MN), anti-CEACAM1 CC1 from Kathryn Holmes, (University of Colorado, Denver, CO), and anti-VEGF-A (2G11-2A05) and anti-Gr1 (RB6–8C5) from Biolegend (San Diego, CA). The isotype control for the anti-Bv8 and anti-CEACAM1 treatments was murine anti-human CD33 (IgG1 produced in-house at City of Hope).

Tumor cell lines and animals

B16F10 and MC38 cells were from ATCC and maintained in DMEM supplemented with 10% FBS. Ceacam1$^{-/-}$ mice were provided by Dr. Beauchemin (McGill University, Montreal, Canada). B16 tumor cells 10^5 in 100μl PBS were injected s.c. into 8–12-wk-old WT or transgenic mice, and tumor sizes measured every 2 to 3 days.

Isolation of tumor-infiltrating immune cells

Tumors were cut into 1–2 mm^3 and digested for 30 min at 37°C by collagenase D/DNase I (Roche) in DMEM. Cell suspensions were filtered through a 70μm cell strainer, and dead cells were removed by centrifugation at 600 g over a Histopaque gradient (Sigma-Aldrich).

Bone marrow reconstitution assay

Bone marrow from C57BL/6 and Ceacam1$^{-/-}$ mice (donors) was transferred into Ceacam1$^{-/-}$ and C57BL/6 lethally irradiated recipients. Retroviral vectors were constructed as previously described (13). Briefly, 5-Fluorouracil (5 mg/mouse) was injected i.p. into Ceacam1$^{-/-}$ mice and bone marrow stem cells harvested 5 days later and cultured in 10% FBS DMEM supplemented with 20 ng/ml IL-3, 50 ng/ml IL-6, and SCF for 24 hr. Bone marrow stem cells were transduced with retroviral vectors and after 2–3 days were sorted as GFP-positive cells. Lethally irradiated Ceacam1$^{-/-}$ mice were i.v. injected with sorted cells.

In vivo Matrigel angiogenesis assay

B16 cells (5×10^4) in 600 μl of growth factor–reduced Matrigel (BD Biosciences) were injected into wild type or Ceacam1$^{-/-}$ mice. Matrigel plugs were dissected 6 d later and analyzed for hemoglobin content by colorimetry using the Drabkin reagent (Sigma-Aldrich) or stained for CD31 or Gr1.

Coinjection of tumor cells with Gr1$^+$CD11b$^+$ myeloid cells

CD11b$^+$Gr1$^+$ myeloid cells from spleen of tumor-bearing Ceacam1$^{-/-}$ and WT mice were sorted using AutoMACS. Enriched Gr1+CD11b+ cells (2×10^5) from Ceacam1$^{-/-}$ or WT mice were mixed with B16F10 cells (1×10^5/mouse) and injected s.c. into C57BL/6 mice. At day 2 and 4, additional Gr1$^+$CD11b$^+$ cells were sorted and injected into the tumor site.

Immunohistochemistry and immunofluorescence

For immunohistochemical analysis, the primary antibody was rat anti- mouse CD31 1/25 (BD Pharmingen 550274) and the secondary rabbit anti-rat secondary antibody from Vector Labs. For immunofluoresent staining, 5-μm sections of flash-frozen tumor specimens were fixed in acetone, permeabilized with methanol, incubated with rat anti-mouse Gr1$^+$ or rat

anti-mouse CD31 in PBS supplemented with 10% goat serum and 2.5% mouse serum, and detected with goat anti-rat conjugated Alexa Fluor 546 or 488 (Invitrogen).

Anti-Gr1, anti-Bv8, anti-VEGF-A, anti-G-CSF and anti-CEACAM1 antibody treatments

B16F10 cells ($3-4 \times 10^5$) in 100 μl PBS were injected s.c. in Ceacam1$^{-/-}$ or C57BL/6 mice. Fifty μg of monoclonal rat anti-Gr1 antibody (RB6–8C5) in 100 μl PBS was injected i.p. into each mouse at day –1, day 0 (1 hour before tumor cells), and at days 2, 4, 6, 8, and 10. Mouse anti-Bv8 mAbs 2B9 plus 3F1 or isotype controls were administered (250 μg, i.p. twice a week). Rat anti-VEGF-A mAb (2G11-2A05) alone or in combination with anti-Bv8 mAbs was administered at 100 μg/mouse by i.p. twice a week.Anti-mouse G-CSF mAb (MAB414) and the matching isotype control were administered (10 μg/day) and anti-CEACAM1 and isotype control (40 μg every other day).

Cell Sorting and Flow Cytometric Analysis

Spleen or bone marrow cells prepared in PBS supplemented with 2% FBS were incubated with biotin conjugated anti-Gr1$^+$ plus biotin magnetic beads and sorted by AutoMACS. Single cell suspensions were labeled with FITC or APC-conjugated anti-Gr1, APC-Cy7-conjugated anti- mouse CD11b and analyzed on a FACS Canto II (BD Biosciences).

G-CSF treatment and RT- PCR

Cells (2×10^6 Gr1$^+$CD11b$^+$) were cultured for 4h with G-CSF (50 ng/ml). RNA was isolated by RNeasy (Qiagen), reverse transcripts by a cDNA synthesis Kit (SABiosciences), and RT-PCR by SYBR Green supermix (SABiosciences) on a Bio-Rad IQ5 with GAPDH controls.

Immunoblots, ELISA and statistical analysis

Cells (5×10^6 Gr1$^+$CD11b$^+$) ± G-CSF treatment (50 ng/mL, 6h-8h) were lysed using RIPA buffer (Sigma) supplemented with 4 mM Na$_3$VO$_4$, 50 mM NaF and 1 mM PMSF and immunoblotted with anti-Bv8. Tumos from C57BL/6 and Ceacam1$^{-/-}$ mice were homogenized, filtered (70 μm strainer), centrifuged and cultured (2×10^6) in DMEM supplemented with 10% FBS overnight. Supernatants were analyzed for G-CSF and VEGF using ELISA kits (R&D Systems). Two-tailed p-values were calculated by the unpaired t test using Prism software (GraphPad Software, Inc.).

Results

Enhanced tumor growth and angiogenesis in CEACAM1$^{-/-}$ mice

Although CEACAM1 is recognized as a tumor suppressor gene due to its down-regulation in many solid tumors including colon (15, 27, 28), prostate (16) and breast (17), the opposite is found in melanoma (18, 29) and lung cancer (30, 31). Notably, few studies focused on the role of CEACAM1 expression in the tumor microenvironment, including immune cells that promote tumor growth and angiogenesis. To approach this problem, we selected a tumor model in immune competent mice that had either wild type expression or no expression of CEACAM1. C57BL/6 or Ceacam1$^{-/-}$ mice were challenged with the syngeneic melanoma cell line B16F10. Tumor growth was enhanced significantly (about two-fold) in Ceacam1$^{-/-}$ compared to wild type mice (Figure 1A). Since tumor growth is dependent on new blood vessel formation, we determined if the enhanced tumor growth in Ceacam1$^{-/-}$ mice was associated with increased tumor angiogenesis. Indeed, tumor blood vessel density was about two-fold higher in Ceacam1$^{-/-}$ mice compared to tumors in wild type mice (Figure 1B and C). To confirm that angiogenesis is enhanced in the Ceacam1$^{-/-}$ microenvironment, we performed an *in vivo* Matrigel plug angiogenesis assay in recipient C57BL/6 or Ceacam1$^{-/-}$

mice (Figure 1D). The hemoglobin content (Figure 1E) as well as vascularity (Figure 1F) was significantly elevated in Matrigel plugs from Ceacam1$^{-/-}$ mice, indicating that angiogenesis is enhanced in Ceacam1$^{-/-}$ mice. Immunofluorescent staining of CD31 positive endothelia is shown in Figure S1.

Enhanced tumor growth and angiogenesis is dependent on bone marrow-derived cells but independent of T and B cells

Bone marrow derived myeloid cells such as macrophages, granulocytes, and dendritic cells play a critical role in mediating tumor growth and angiogenesis (32). To determine if bone marrow derived cells are responsible for the enhanced tumor growth and angiogenesis in CEACAM1$^{-/-}$ mice, we generated bone marrow chimeras. Ceacam1$^{-/-}$ and wild type mice were lethally irradiated and reconstituted with bone marrow from either wild type or Ceacam1$^{-/-}$ mice, respectively. After 8 weeks, B16 melanoma cells were injected s.c. in the bone marrow reconstituted mice. Tumor growth in wild type recipients with Ceacam1$^{-/-}$ bone marrow was enhanced compared to that in Ceacam1$^{-/-}$ recipients with wild type bone marrow (Figure 2A). Tumor growth was dependent on the donor bone marrow, rather than the recipient. Consistently, immunohistochemical analysis revealed increased numbers of blood vessels in wild type recipients with Ceacam1$^{-/-}$ bone marrow compared to Ceacam1$^{-/-}$ recipients with wild type bone marrow (Figure 2B and C). These results demonstrate that bone marrow derived cells are responsible for the enhanced tumor growth in Ceacam1$^{-/-}$ mice. Since the bone marrow reconstitution study includes T- and B-cell progenitors and these cell express CEACAM1 when activated (14), we crossed the CEACAM1$^{-/-}$ mice into the Rag1$^{-/-}$ background. When these mice were challenged with B16 melanoma cells, tumor growth was enhanced about two-fold compared to Rag1$^{-/-}$ mice (Figure 2D). Immunohistochemical analysis of tumor tissue showed that tumor angiogenesis was increased in Ceacam1$^{-/-}$ Rag1$^{-/-}$ compared to Rag1$^{-/-}$ mice (Figure 2E and F). Since Rag$^{-/-}$ mice have normal expression of CEACAM1 in their myeloid cells, these data suggest that increased tumor growth in Ceacam1$^{-/-}$ mice is independent of T- and B- cells.

Inhibitory regulation of tumor growth by Ceacam1 is dependent on its ITIMs

The ITIM domains on the long cytoplasmic domain isoform of CEACAM1 perform an inhibitory role in the immune system by recruiting SHP-1/2 phosphatases that attenuate signaling pathways in lymphocytes (14, 33). When the tyrosines in the ITIMs were mutated to Phe or Ala, their inhibitory activity was abolished (33). Previously, we have shown that the ITIMs in the long cytoplasmic domain isoform of CEACAM1 in granulocytes inhibit granulopoiesis by recruiting SHP-1 and inhibiting activated G-CSFR signaling (13). Since our data suggest that CEACAM1 is an inhibitory mediator for tumor growth and angiogenesis in the B16 melanoma tumor model, it was important to demonstrate that CEACAM1 inhibits tumor growth through its ITIM domains. Therefore, we reconstituted wild type or Tyr mutated long cytoplasmic isoforms of CEACAM1 into Ceacam1$^{-/-}$ mouse bone marrow. As a control, we also reconstituted Ceacam1$^{-/-}$ mouse bone marrow with the short cytoplasmic domain isoform which lacks ITIMs. We found that only the long cytoplasmic domain isoform of CEACAM1 was able to restore tumor growth to levels compared to wild-type mice (Figure S2A), while the short cytoplasmic domain isoform of CEACAM1 did not play a role in tumor growth inhibition (Figure S2B). Furthermore, mutation of the ITIMs on the long cytoplasmic domain isoform of CEACAM1 failed to suppress tumor growth (Figure S2A). Thus, bone marrow reconstitution analysis indicates that the ITIMs of the long cytoplasmic domain isoform of CEACAM1 are responsible for its role in tumor growth inhibition.

Enhanced infiltration of Gr1⁺ CD11b⁺ myeloid cells into tumors of Ceacam1⁻/⁻ mice

Since we have shown enhanced tumor growth and angiogenesis are mediated by bone marrow-derived cells, we investigated which population of bone marrow-derived cells plays this role. More than 80% of tumor-associated immune cells are $Gr1^+$ $CD11b^+$ myeloid cells (4). $Gr1^+CD11b^+$ cells have immunosuppressive functions ascribed to inhibition of the functions of T and NK cells, and promotion of T-reg cell proliferation (34, 35). In addition, $Gr1^+CD11b^+$ myeloid cells are critical promoters of tumor angiogenesis (32). Therefore, it was important to determine if enhanced tumor growth and angiogenesis in Ceacam1⁻/⁻ mice was related to enhanced infiltration of $Gr1^+CD11b^+$ myeloid cells into the tumor microenvironment. Tumor tissues were analyzed by immunofluorescence staining using anti-$Gr1^+$ antibody to visualize tumor infiltrating $Gr1^+$ myeloid cells. Since over 90% of $Gr1^+$ cells are also $CD11b^+$, the population of $Gr1^+$ cells is representative of $Gr1^+CD11b^+$ cells (36). Immunofluorescence analysis showed that higher numbers of $Gr1^+$ cells infiltrated into tumors of Ceacam1⁻/⁻ compared to wild type mice (Figure 3A and B). Flow cytometric analysis of dissociated tumor tissue also confirmed that the population of $Gr1^+CD11b^+$ myeloid cells in tumor is higher in Ceacam1⁻/⁻ compared to wild type mice (Figure 3C, Figure S3). Furthermore, the percentage of $Gr1^+CD11b^+$ myeloid cells are significantly increased in spleen, peripheral blood and bone marrow of Ceacam1⁻/⁻ mice, indicating that production and the migration of these cells into the periphery is increased (Figure 3C). Flow cytometric analysis also showed that infiltration of $Gr1^+CD11b^+$ cells in tumor and blood in wild type recipients reconstituted with Ceacam1⁻/⁻ bone marrow was elevated compared to that in Ceacam1⁻/⁻ recipients with wild type bone marrow, demonstrating that the higher numbers of infiltrating $Gr1^+CD11b^+$ in tumors and peripheral organs is dependent on their bone marrow origin (Figure 3D). These data also suggest that the Ceacam1⁻/⁻ $Gr1^+CD11b^+$ cells have an enhanced ability to migrate into peripheral tissues and might be responsible for enhanced tumor growth and angiogenesis. Consistently, the population of $Gr1^+CD11b^+$ cells in tumor, spleen, blood and bone marrow is higher in Ceacam1⁻/⁻Rag1⁻/⁻ mice than in Rag1⁻/⁻ mice, indicating that the enhanced infiltration of these cells in Ceacam1⁻/⁻ mice is independent of T and B cells (Figure 3D). A similar increase in infiltrating Gr1+ cells was seen in Matrigel plugs in Ceacam1⁻/⁻ mice (Figure 3E). When tumors were stained for NK cells, the percent activated NK cells were lower in the Ceacam1⁻/⁻ (2.7%) than in WT mice (3.2%) (data not shown).

Gr1⁺CD11b⁺ myeloid cells are necessary and sufficient for enhanced tumor growth and angiogenesis in Ceacam1⁻/⁻ mice

Since tumor infiltrating $Gr1^+CD11b^+$ myeloid cells were shown to play an important role in promoting tumor growth and angiogenesis (2) and their numbers are increased in Ceacam1⁻/⁻ mice, we determined if $Gr1^+CD11b^+$ cells in Ceacam1⁻/⁻ mice were functionally more aggressive compared to those in wild type mice. B16 melanoma cells mixed with $Gr1^+CD11b^+$ cells from the spleens of either tumor-bearing Ceacam1⁻/⁻ or wild type mice were implanted into wild type mice and tumor growth measured. As expected, tumor growth was significantly increased in recipients with a mixture of B16 melanoma cells and either wild type or Ceacam1⁻/⁻ $Gr1^+CD11b^+$ cells, compared to the recipients with B16 cells alone (Figure 4A). However, recipients with mixture of B16 melanoma cells and Ceacam1⁻/⁻ $Gr1^+CD11b^+$ cells had enhanced tumor growth compared to recipients with mixture of B16 and $Gr1^+CD11b^+$ cells from wild type mice (Figure 4A). Immunohistochemical analysis of tumor tissue showed enhanced numbers of blood vessels in recipients with a mixture of B16 and $Gr1^+CD11b^+$ myeloid cells compared to recipients with B16 melanoma cells alone (Figure 4B and 4C). There were even more blood vessels in recipients with a mixture of B16 and $Gr1^+CD11b^+$ cells enriched from Ceacam1⁻/⁻ mice compared to recipients with a mixture of B16 and $Gr1^+CD11b^+$ cells enriched from wild type mice (Figure 4B and 4C). These results demonstrate that $Gr1^+CD11b^+$ myeloid cells

alone are responsible for enhanced tumor growth and angiogenesis. Furthermore, $Gr1^+CD11b^+$ myeloid cells from $Ceacam1^{-/-}$ tumor-bearing mice more potently promote tumor growth and angiogenesis than those from tumor-bearing wild type mice.

To further demonstrate the importance of these cells, we performed cell depletion studies using anti-$Gr1^+$ antibody in $Ceacam1^{-/-}$ or wild type mice. In both cases, depletion of $Gr1^+CD11b^+$ cells significantly reduced tumor growth and angiogenesis (Figure 4D, 4E and 4F). After depletion, there was no significant difference of tumor growth in wild type and $Ceacam1^{-/-}$ mice. Those data indicate $Gr1^+CD11b^+$ cells are necessary and sufficient to mediate the enhanced tumor growth and angiogenesis observed in $Ceacam1^{-/-}$ mice.

Elevated Bv8 production in $Ceacam1^{-/-}$ $Gr1^+CD11b^+$ myeloid cells

$Gr1^+CD11b^+$ myeloid cells mediate tumor angiogenesis by producing pro-angiogenic factors, especially Bv8 (2, 5, 32). Bv8 expression in the bone marrow of tumor-bearing mice is positively regulated by G-CSF (5), the major cytokine responsible for granulopoiesis. Since we found that CEACAM1 is a negative regulator of the G-CSFR signaling pathway in myeloid progenitor cells (13), we thought it likely that CEACAM1 would regulate G-CSF mediated Bv8 expression. Previously, we showed that after G-CSF binds to G-CSFR, CEACAM1 associates with G-CSFR recruiting SHP-1, which in turn, dephosphorylates activated G-CSFR and Stat3 signaling, resulting in the attenuation of granulopoiesis (13). Given these findings, we determined if CEACAM1 negatively regulates G-CSF driven Bv8 production in $Gr1^+CD11b^+$ myeloid cells, thus accounting for the mechanism of increased tumor growth and angiogenesis in $Ceacam1^{-/-}$ mice. First, we found that G-CSF levels were elevated in tumors from $Ceacam1^{-/-}$ mice (Figure 5A). Second, we found that VEGF levels were similar in tumors from wild type or $Ceacam1^{-/-}$ mice (Figure 5A), indicating VEGF does not play an important role in mediating enhanced tumor angiogenesis in $Ceacam1^{-/-}$ mice. $Gr1^+CD11b^+$ myeloid cells isolated from $Ceacam1^{-/-}$ spleens or tumors showed higher Bv8 mRNA transcript levels compared to wild type controls (Figure 5B). However, there was no significant change of VEGF mRNA transcripts in wild type or $Ceacam1^{-/-}$ $Gr1^+CD11b^+$ cells from tumor or spleen (Figure 5C). Since the expression of Bv8 is regulated by G-CSF, we determined if the G-CSF-Bv8 pathway in $Ceacam1^{-/-}$ myeloid cells was more active compared to wild type controls. We enriched bone-marrow $Gr1^+CD11b^+$ or $Gr1^-CD11b^-$ cells from $Ceacam1^{-/-}$ and wild-type mice, and incubated them in the presence or absence of G-CSF. The results demonstrated that G-CSF triggered Bv8 expression specifically in $Gr1^+CD11b^+$ myeloid cells (Figure 5D). Also WT $Gr1^-CD11b^-$ cells make negligible amounts of Bv8 mRNA in response to G-CSF (Figure 5D). The Bv8 mRNA transcript level is about 7-fold higher in $Ceacam1^{-/-}$ $Gr1^+CD11b^+$ myeloid cells compared to wild type $Gr1^+CD11b^+$ myeloid cells in response to the same dose of G-CSF (Figure 5D). Western-blot analysis confirmed that the expression of Bv8 protein in $Ceacam1^{-/-}$ $Gr1^+CD11b^+$ myeloid cells was higher compared to wild type controls with G-CSF treatment (Figure 5E). Importantly, in the absence of G-CSF, there was no significant difference in Bv8 protein expression in $Ceacam1^{-/-}$ versus wild type $Gr1^+CD11b^+$ myeloid cells (Figure 5E). As expected, $Gr1^-CD11b^-$ cells make negligible amounts of Bv8 protein (data not shown).

Anti-G-CSF, anti-Bv8 or anti-VEGF treatments delayed tumor growth and angiogenesis in $CEACAM1^{-/-}$ mice

Tumor-associated $Gr1^+CD11b^+$ cells were increased in $Ceacam1^{-/-}$ mice with concomitant expression of pro-angiogenic factor Bv8 in Gr1+CD11b+ cells from $Ceacam1^{-/-}$ mice. G-CSF, the major up-regulator of Bv8 was also increased in the tumors from $Ceacam1^{-/-}$ mice. To test if elevated Bv8 and G-CSF were responsible for the enhanced tumor growth and angiogenesis in $Ceacam1^{-/-}$ mice, we treated $Ceacam1^{-/-}$ tumor-bearing mice with anti-

Bv8 or anti-G-CSF antibody. We found anti-Bv8 antibody treatment significantly reduced the tumor growth in Ceacam1$^{-/-}$ mice to the level in controls (Figure 6A). We also found that anti-Bv8 antibody treatment remarkably reduced both tumor angiogenesis and tumor-associated Gr1$^+$ infiltrates in Ceacam1$^{-/-}$ mice (Figure 6B, 6C and 6D). Thus, our data indicate that Bv8 plays a critical role in mediating the increased tumor growth and angiogenesis in Ceacam1$^{-/-}$ mice in B16F10 melanoma model.

Similarly, anti-G-CSF antibody treatment significantly reduced tumor growth and the infiltration of Gr1$^+$CD11b$^+$ myeloid cells in tumor bearing Ceacam1$^{-/-}$ mice, but not in wild type mice (Figure S4A). The number of blood vessels in tumors from Ceacam1$^{-/-}$ mice decreased with anti-G-CSF treatment, but not in wild type mice (Figure S4B and 4C). Anti-G-CSF treatment reduced the population of Gr1$^+$CD11b$^+$ in the bone marrow of Ceacam1$^{-/-}$ and wild type mice, while the number of Gr1$^+$CD11b$^+$ cells in the spleen was not significantly reduced in wild type compared to Ceacam1$^{-/-}$ mice (Figure S4D), which may explain why tumor growth was not reduced in response to anti-G-CSF treatment in wild type mice. These results indicate that the increased G-CSF-Bv8 signaling in Ceacam1$^{-/-}$ mice plays a major role in mediating the increased tumor growth in Ceacam1$^{-/-}$ mice, indicating that CEACAM1 is a negative regulator in this pathway.

Although VEGF mRNA levels are similar in B16 tumors from WT and Ceacam1$^{-/-}$ mice (Figure 5C), the production of VEGF is likely to play some role in tumor growth (i.e., tumor growth is reduced not eliminated in anti-Bv8 treated mice). Indeed, anti-VEGF treatment of Ceacam1$^{-/-}$ mice bearing B16 tumors significantly reduced tumor size (Figure 7A) as well as tumor vasculature (Figure 7B) and the numbers of infiltrating Gr1$^+$ cells (Figure 7C). However, since treatment of tumor bearing Ceacam1$^{-/-}$ mice with a combination of anti-Bv8 and anti-VEGF antibodies had no additive effects (Figure 7A), it is likely that they operate independently of each other in this animal model.

Anti-CEACAM1 treatment delayed tumor growth and angiogenesis in wild type mice

In order to test if CEACAM1 a potential therapeutic target for cancer treatment, we treated wild type tumor-bearing mice with an anti-CEACAM1 antibody. Indeed, we found that anti-CEACAM1 antibody treatment reduced both tumor growth and angiogenesis (Figure S5A S5B and S5C). Since CEACAM1 is predominantly expressed on Gr1$^+$CD11b$^+$ cells, we checked the population of those cells after anti-CEACAM1 antibody treatment and found that the numbers of Gr1$^+$CD11b$^+$ cells were reduced in spleen and blood in response to anti-CEACAM1 antibody treatment (Figure S5D). We conclude that anti-CEACAM1 antibody confers an anti-tumor effect by reduction of Gr1$^+$CD11b$^+$ cell numbers.

Enhanced MC38 colon tumor growth in Ceacam1$^{-/-}$ mice

Since we observed accelerated B16 melanoma tumor growth in Ceacam1$^{-/-}$ mice and CEACAM1 expression has been associated with a poor prognosis in human melanoma (18), it was important to determine if the role of CEACAM1 in myeloid cells was specific to the melanoma tumor model. Therefore, we tested if tumor growth, angiogenesis and the phenotype of infiltrating myeloid cells were similar in a second syngeneic tumor model. The MC38 colon tumor was chosen because CEACAM1 is a tumor suppressor in colon cancer (15, 27). MC38 tumor growth in Ceacam1$^{-/-}$ mice was significantly more aggressive than wild type mice (Figure S7A) with increased blood vessel numbers in tumors from Ceacam1$^{-/-}$ versus wild type mice (Figure S7B and S7C). Similar to the B16 melanoma model, infiltration of Gr1+CD11b+ myeloid cells was increased in Ceacam1$^{-/-}$ mice (Figure S7D, S7E and S7F). Therefore, lack of expression of CEACAM1 in Ceacam1$^{-/-}$ host myeloid cells enhances tumor growth in a second model system that is usually associated with a tumor suppressor role for CEACAM1. We conclude that CEACAM1 mediated

inhibition of myeloid cell infiltration and tumor angiogenesis is not specific to the B16 melanoma tumor model and may be a general feature of the regulated role of myeloid cells in tumor development.

Discussion

Although the cell-cell adhesion molecule CEACAM1 is down-regulated in a number of cancers, including prostate (16), breast (17), and colon (27, 28), the precise mechanism of its tumor suppressive activity is unclear. In fact, there is evidence in several cancers such as melanoma (19) and lung (31) that CEACAM1 expression correlates with a poor prognosis. Although most research has focused on the role of Ceacam1 in cancer cells, the role of Ceacam1 in immune cell-mediated tumorigenesis and tumor angiogenesis is less studied. For example, bone marrow derived lymphocytes and myeloid cells are known to play critical roles in tumor growth and angiogenesis. In support of this idea, we show in the B16 melanoma tumor model that an enhanced tumor growth and angiogenesis in Ceacam1$^{-/-}$ mice is mediated by bone marrow cells using a reverse bone marrow transplantation assay performed between wild type and ceacam1$^{-/-}$ mice. Furthermore we found that Gr1$^+$CD11b$^+$ cells were increased in tumor, spleen, blood and bone marrow in tumor bearing Ceacam1$^{-/-}$ mice. Co-injection Gr1$^+$CD11b$^+$ cells with tumor cells or depletion of Gr1$^+$CD11b$^+$ cells verified the specific ability of Gr1$^+$CD11b$^+$ cells to mediate both tumor growth and angiogenesis. These results agree with previous findings that show infiltration of Gr1$^+$CD11b$^+$ cells mediates VEGF-independent tumor angiogenesis in various tumor models (4) and that Bv8 may be the chemo-attractant for Gr1$^+$ cells (6). The higher numbers of infiltrating Gr1$^+$CD11b$^+$ in tumors in our Ceacam1$^{-/-}$ tumor model are similar to those found in tumor models that are refractory to anti-VEGF treatment (4). Although, we found VEGF levels in the tumor microenvironment and Gr1$^+$CD11b$^+$ cells in Ceacam1$^{-/-}$ mice were similar to those in wild type mice, anti-VEGF therapy also reduced tumor angiogenesis in Ceacam1$^{-/-}$ mice. Similar to the finding that pro-angiogenic factor Bv8 and its regulator G-CSF are enhanced in Gr1$^+$CD11b$^+$ cell-mediated tumors refractory to anti-VEGF treatment (7), we found elevated Bv8, G-CSF and tumor-associated myeloid cells in the tumor-bearing Ceacam1$^{-/-}$ mice. Blocking Bv8 and G-CSF in Ceacam1$^{-/-}$ mice reduced tumor growth and angiogenesis to control levels.

It has been shown that G-CSF mediates the secretion of Bv8 in Gr1$^+$CD11b$^+$ cells. Thus, both anti-G-CSF and anti-Bv8 treatments have been shown to reduce tumor growth and angiogenesis (5, 7). Since our group previously found that CEACAM1 is a negative regulator of the G-CSFR-Stat3 pathway in myeloid progenitor cells (13) and G-CSF mediates Bv8 production, we hypothesized CEACAM1 also regulates this pathway. In the case of myeloid progenitors, G-CSF recruits CEACAM1 to G-CSFR where both G-CSFR and CEACAM1 are phosphorylated. The phosphorylation of CEACAM1 on its ITIMs recruits the inhibitory phosphatase SHP-1, which in turn, dephosphorylates G-CSFR and its downstream signaling mediator Stat3 (13). In agreement with the role of CEACAM1 in negatively regulating the G-CSFR-Stat3 pathway in myeloid cells, our current study demonstrates that CEACAM1 is also a negative regulator of the G-CSF-Bv8 axis in Gr1$^+$CD11b$^+$ myeloid cells. A prediction of this role for CEACAM1 is elevated Bv8 expression in Ceacam1$^{-/-}$ Gr1$^+$CD11b$^+$ myeloid cells. Proof that this role is provided by the ITIMs on CEACAM1 was shown by bone marrow reconstitution of wild type long isoform, but not ITIM mutants or the short form isoform of CEACAM1 lacking ITIMs can reduce tumor growth and angiogenesis to wild type levels. Thus, the ITIM domains on the long isoform of CEACAM1 are responsible for its inhibitory activity. These results not only emphasize the important role of G-CSF in stimulating Bv8 mediated tumor angiogenesis, but also the requirement for its negative regulation by CEACAM1. In addition, this role of CEACAM1 may apply to other cells that express CEACAM1 and utilize the G-CSF

pathway. We conclude that tumor angiogenesis, like angiogenesis in general, must be tightly controlled by both positive and negative regulators.

Distinct functions of CEACAM1 in angiogenesis have been explored in different cell types and in different models. In endothelial cells, CEACAM1 activates angiogenesis by re-organizing by cytoskeleton and integrin signaling (24, 37). Deletion of CEACAM1 in primary murine lung endothelial cells induces defective vascular permeability (25), perhaps indicating a role for CEACAM1 in blood vessel stability. Down regulation of CEACAM1 in epithelial cells in prostate intraepithelial neoplasia was followed by enhanced vascularization of prostate tumors, a result attributed to an unknown secreted factor produced by CEACAM1 positive prostate epithelial cells that inhibits angiogenesis (38). In our own study, we found that CEACAM1 is required for vasculogenesis in embryonic stem cells (26). Vascular sprouting was inhibited by either anti-CEACAM1 or anti-PECAM1 antibodies, emphasizing that both receptors are required for neo-vascularization. Anti-CEACAM1 antibodies were able to inhibit tumor growth and angiogenesis in our B16 melanoma model by reducing the $Gr1^+CD11b^+$ cells. Regarding the effect of CEACAM1 in immune cell-mediated angiogenesis, it was reported that CEACAM1 is required for $Ly6C^+CD11b^+$ monocytes-mediated-angiogenesis in inflammation in a model of cutaneous leishmaniasis (23). In contrast, in our melanoma tumor model, we found that $Gr1^+CD11b^+$ myeloid cells from $Ceacam1^{-/-}$ mice have an enhanced ability to promote tumor angiogenesis, indicating that Ceacam1 negatively regulates tumor angiogenesis. Although these studies may suggest opposing roles of CEACAM1 in wound healing or inflammation associated angiogenesis versus tumor angiogenesis, it can be argued that they are all consistent with a role for CEACAM1 in controlling the degree of angiogenesis by regulation of G-CSFR-Stat3 signaling. Even in our tumor model, CEACAM1 positive myeloid cells are able to sustain tumor growth. It is only in the absence of CEACAM1 that tumor growth is enhanced by the myeloid cells. Since CEACAM1 is able to prevent unrestrained tumor growth, it may play a similar role in angiogenesis in general. To sort out these apparent discrepancies, a complete analysis of the signaling pathways utilized is necessary, especially in VEGF-independent angiogenesis.

In summary, our findings demonstrate the significance of the inhibitory regulation of $Gr1^+CD11b^+$ myeloid cell-mediated tumor growth and angiogenesis by CEACAM1 through the G-CSF-Bv8 axis. The fact that antibody mediated therapy against Bv8 and G-CSF, as well as CEACAM1, reduces tumor growith underscores the identification of CEACAM1 as a novel therapeutic potential target for tumor angiogenesis.

Supplementary Material

Refer to Web version on PubMed Central for supplementary material.

Acknowledgments

References

1. Shojaei F, Ferrara N. Refractoriness to antivascular endothelial growth factor treatment: role of myeloid cells. Cancer Res. 2008; 68:5501–5504. [PubMed: 18632597]

2. Yang L, DeBusk LM, Fukuda K, Fingleton B, Green-Jarvis B, Shyr Y, et al. Expansion of myeloid immune suppressor Gr+CD11b+ cells in tumor-bearing host directly promotes tumor angiogenesis. Cancer Cell. 2004; 6:409–421. [PubMed: 15488763]

3. Kujawski M, Kortylewski M, Lee H, Herrmann A, Kay H, Yu H. Stat3 mediates myeloid cell-dependent tumor angiogenesis in mice. J Clin Invest. 2008; 118:3367–3377. [PubMed: 18776941]

4. Shojaei F, Wu X, Malik AK, Zhong C, Baldwin ME, Schanz S, et al. Tumor refractoriness to anti-VEGF treatment is mediated by CD11b+Gr1+ myeloid cells. Nat Biotechnol. 2007; 25:911–920. [PubMed: 17664940]

5. Shojaei F, Wu X, Zhong C, Yu L, Liang XH, Yao J, et al. Bv8 regulates myeloid-cell-dependent tumour angiogenesis. Nature. 2007; 450:825–831. [PubMed: 18064003]

6. Kowanetz M, Wu X, Lee J, Tan M, Hagenbeek T, Qu X, et al. Granulocyte-colony stimulating factor promotes lung metastasis through mobilization of Ly6G+Ly6C+ granulocytes. Proc Natl Acad Sci U S A. 2010; 107:21248–21255. [PubMed: 21081700]

7. Shojaei F, Wu X, Qu X, Kowanetz M, Yu L, Tan M, et al. G-CSF-initiated myeloid cell mobilization and angiogenesis mediate tumor refractoriness to anti-VEGF therapy in mouse models. Proc Natl Acad Sci U S A. 2009; 106:6742–6747. [PubMed: 19346489]

8. LeCouter J, Zlot C, Tejada M, Peale F, Ferrara N. Bv8 and endocrine gland-derived vascular endothelial growth factor stimulate hematopoiesis and hematopoietic cell mobilization. Proc Natl Acad Sci U S A. 2004; 101:16813–16818. [PubMed: 15548611]

9. Shojaei F, Singh M, Thompson JD, Ferrara N. Role of Bv8 in neutrophil-dependent angiogenesis in a transgenic model of cancer progression. Proc Natl Acad Sci U S A. 2008; 105:2640–2645. [PubMed: 18268320]

10. Zhong C, Qu X, Tan M, Meng YG, Ferrara N. Characterization and regulation of bv8 in human blood cells. Clin Cancer Res. 2009; 15:2675–2684. [PubMed: 19336519]

11. LeCouter J, Ferrara N. EG-VEGF and Bv8. a novel family of tissue-selective mediators of angiogenesis, endothelial phenotype, and function. Trends Cardiovasc Med. 2003; 13:276–282. [PubMed: 14522467]

12. LeCouter J, Lin R, Tejada M, Frantz G, Peale F, Hillan KJ, et al. The endocrine-gland-derived VEGF homologue Bv8 promotes angiogenesis in the testis: Localization of Bv8 receptors to endothelial cells. Proc Natl Acad Sci U S A. 2003; 100:2685–2690. [PubMed: 12604792]

13. Pan H, Shively JE. Carcinoembryonic antigen-related cell adhesion molecule-1 regulates granulopoiesis by inhibition of granulocyte colony-stimulating factor receptor. Immunity. 2010; 33:620–631. [PubMed: 21029969]

14. Gray-Owen SD, Blumberg RS. CEACAM1: contact-dependent control of immunity. Nat Rev Immunol. 2006; 6:433–446. [PubMed: 16724098]

15. Kunath T, Ordonez-Garcia C, Turbide C, Beauchemin N. Inhibition of colonic tumor cell growth by biliary glycoprotein. Oncogene. 1995; 11:2375–2382. [PubMed: 8570189]

16. Tilki D, Irmak S, Oliveira-Ferrer L, Hauschild J, Miethe K, Atakaya H, et al. CEA-related cell adhesion molecule-1 is involved in angiogenic switch in prostate cancer. Oncogene. 2006; 25:4965–4974. [PubMed: 16568082]

17. Gencheva M, Chen CJ, Nguyen T, Shively JE. Regulation of CEACAM1 transcription in human breast epithelial cells. BMC Mol Biol. 2010; 11:79. [PubMed: 21050451]

18. Ebrahimnejad A, Streichert T, Nollau P, Horst AK, Wagener C, Bamberger AM, et al. CEACAM1 enhances invasion and migration of melanocytic and melanoma cells. Am J Pathol. 2004; 165:1781–1787. [PubMed: 15509546]

19. Markel G, Ortenberg R, Seidman R, Sapoznik S, Koren-Morag N, Besser MJ, et al. Systemic dysregulation of CEACAM1 in melanoma patients. Cancer Immunol Immunother. 2010; 59:215–230. [PubMed: 19633846]

20. LeBlanc S, Arabzadeh A, Benlolo S, Breton V, Turbide C, Beauchemin N, et al. CEACAM1 deficiency delays important wound healing processes. Wound Repair Regen. 2011; 19:745–752. [PubMed: 22092845]

21. Chen Z, Chen L, Baker K, Olszak T, Zeissig S, Huang YH, et al. CEACAM1 dampens antitumor immunity by down-regulating NKG2D ligand expression on tumor cells. J Exp Med. 2011; 208:2633–2640. [PubMed: 22143889]

22. Ergun S, Kilik N, Ziegeler G, Hansen A, Nollau P, Gotze J, et al. CEA-related cell adhesion molecule 1: a potent angiogenic factor and a major effector of vascular endothelial growth factor. Mol Cell. 2000; 5:311–320. [PubMed: 10882072]

23. Horst AK, Bickert T, Brewig N, Ludewig P, van Rooijen N, Schumacher U, et al. CEACAM1+ myeloid cells control angiogenesis in inflammation. Blood. 2009; 113:6726–6736. [PubMed: 19273835]

24. Horst AK, Ito WD, Dabelstein J, Schumacher U, Sander H, Turbide C, et al. Carcinoembryonic antigen-related cell adhesion molecule 1 modulates vascular remodeling in vitro and in vivo. J Clin Invest. 2006; 116:1596–1605. [PubMed: 16680193]

25. Nouvion AL, Oubaha M, Leblanc S, Davis EC, Jastrow H, Kammerer R, et al. CEACAM1: a key regulator of vascular permeability. J Cell Sci. 2010; 123:4221–4230. [PubMed: 21081647]

26. Gu A, Tsark W, Holmes KV, Shively JE. Role of Ceacam1 in VEGF induced vasculogenesis of murine embryonic stem cell-derived embryoid bodies in 3D culture. Exp Cell Res. 2009; 315:1668–1682. [PubMed: 19285068]

27. Nittka S, Gunther J, Ebisch C, Erbersdobler A, Neumaier M. The human tumor suppressor CEACAM1 modulates apoptosis and is implicated in early colorectal tumorigenesis. Oncogene. 2004; 23:9306–9313. [PubMed: 15568039]

28. Neumaier M, Paululat S, Chan A, Matthaes P, Wagener C. Biliary glycoprotein, a potential human cell adhesion molecule, is down-regulated in colorectal carcinomas. Proc Natl Acad Sci U S A. 1993; 90:10744–10748. [PubMed: 7504281]

29. Markel G, Seidman R, Cohen Y, Besser MJ, Sinai TC, Treves AJ, et al. Dynamic expression of protective CEACAM1 on melanoma cells during specific immune attack. Immunology. 2009; 126:186–200. [PubMed: 18557789]

30. Wang L, Lin SH, Wu WG, Kemp BL, Walsh GL, Hong WK, et al. C-CAM1, a candidate tumor suppressor gene, is abnormally expressed in primary lung cancers. Clin Cancer Res. 2000; 6:2988–2993. [PubMed: 10955775]

31. Dango S, Sienel W, Schreiber M, Stremmel C, Kirschbaum A, Pantel K, et al. Elevated expression of carcinoembryonic antigen-related cell adhesion molecule 1 (CEACAM-1) is associated with increased angiogenic potential in non-small-cell lung cancer. Lung Cancer. 2008; 60:426–433. [PubMed: 18215438]

32. Murdoch C, Muthana M, Coffelt SB, Lewis CE. The role of myeloid cells in the promotion of tumour angiogenesis. Nat Rev Cancer. 2008; 8:618–631. [PubMed: 18633355]

33. Nagaishi T, Pao L, Lin SH, Iijima H, Kaser A, Qiao SW, et al. SHP1 phosphatase-dependent T cell inhibition by CEACAM1 adhesion molecule isoforms. Immunity. 2006; 25:769–781. [PubMed: 17081782]

34. Almand B, Clark JI, Nikitina E, van Beynen J, English NR, Knight SC, et al. Increased production of immature myeloid cells in cancer patients: a mechanism of immunosuppression in cancer. J Immunol. 2001; 166:678–689. [PubMed: 11123353]

35. Gabrilovich DI, Nagaraj S. Myeloid-derived suppressor cells as regulators of the immune system. Nat Rev Immunol. 2009; 9:162–174. [PubMed: 19197294]

36. Nagaraj S, Youn JI, Weber H, Iclozan C, Lu L, Cotter MJ, et al. Anti-inflammatory triterpenoid blocks immune suppressive function of MDSCs and improves immune response in cancer. Clin Cancer Res. 2010; 16:1812–1823. [PubMed: 20215551]

37. Muller MM, Singer BB, Klaile E, Obrink B, Lucka L. Transmembrane CEACAM1 affects integrin-dependent signaling and regulates extracellular matrix protein-specific morphology and migration of endothelial cells. Blood. 2005; 105:3925–3934. [PubMed: 15687237]

38. Volpert O, Luo W, Liu TJ, Estrera VT, Logothetis C, Lin SH. Inhibition of prostate tumor angiogenesis by the tumor suppressor CEACAM1. J Biol Chem. 2002; 277:35696–35702. [PubMed: 12122002]
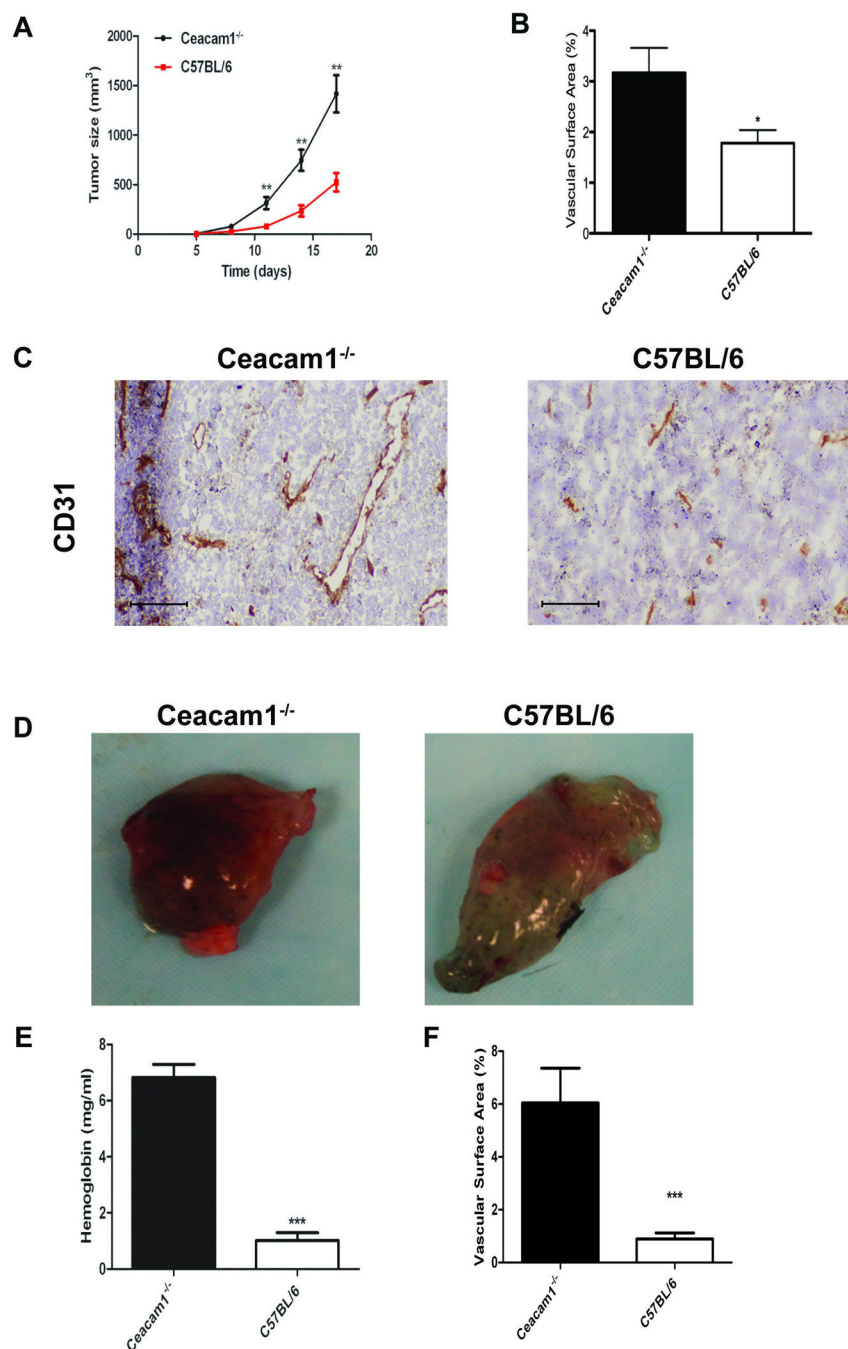
Figure 1. Tumor growth and angiogenesis are enhanced CEACAM1$^{-/-}$ mice
(**A**) B16 tumor cells were injected subcutaneously into C57BL/6 or Ceacam1$^{-/-}$ mice. Data represent mean ± SEM. **0.001<P   0.01 (n=8 mice per group from three independent experiments). (**B**) Blood vessels in tumors were counted based on immunohistological analysis with anti-CD31 of frozen tumor tissue collected from mice in (**A**) after 17 days. More than 8 fields of view were analyzed. Data represent mean ± SEM. ***P   0.001. (**C**) Immunohistochemistry staining of mouse B16 tumor tissue collected from mice in (**A**) after 17 days with anti-CD31 antibody. Bar = 200μm. (**D**) Representative photos of Matrigel plugs isolated from Ceacam1$^{-/-}$ (left) or C57BL/6 (right) mice after 6 days implantation. (**E**)

Quantitation of hemoglobin in Matrigel plugs containing B16 cells from Ceacam1$^{-/-}$ mice or C57B/6 controls. (**F**) Quantitation of vascular surface area in Matrigel plugs containing B16 cells from Ceacam1$^{-/-}$ mice or C57B/6 controls. Data represent mean ± SEM. ***P 0.001 (n=6 mice per group from three independent experiments).
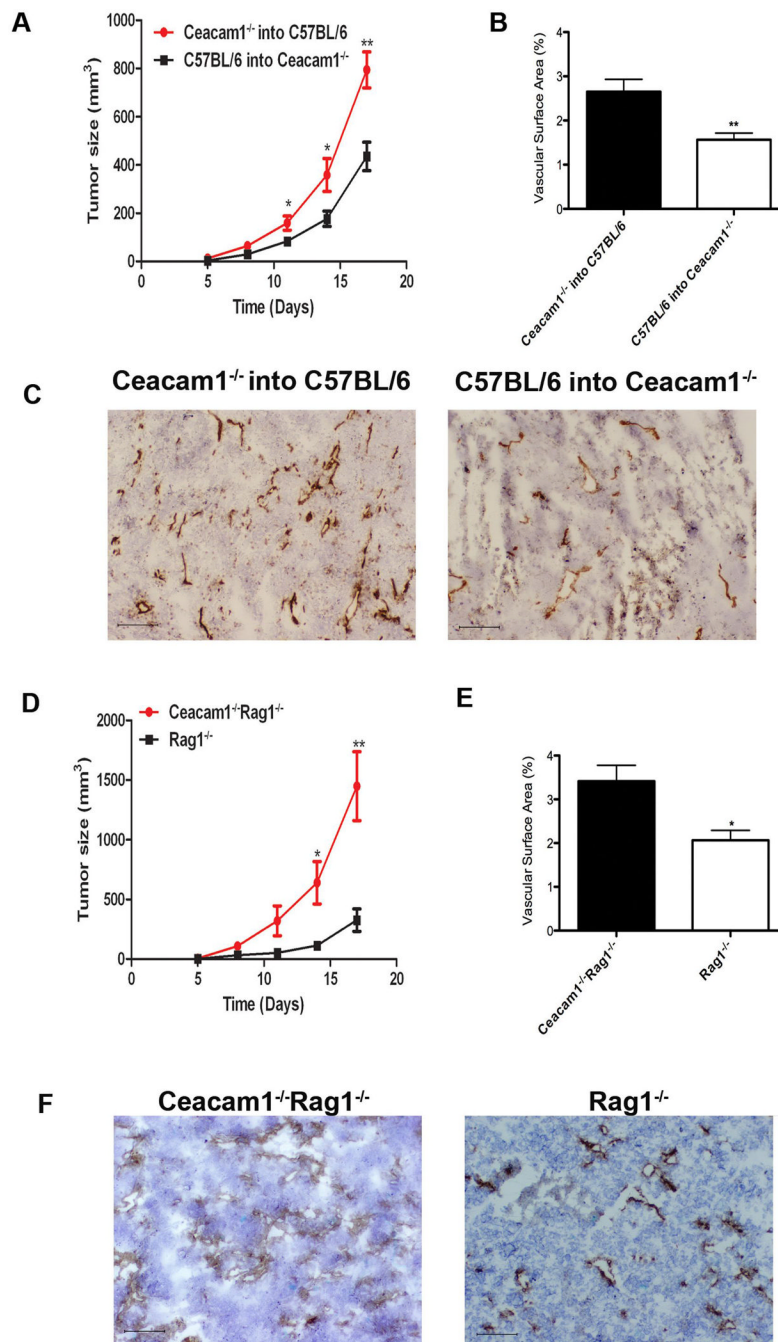
Figure 2. Enhanced tumor growth and angiogenesis is dependent on bone marrow-derived cells but independent of T and B cells

(**A**) Recipient Ceacam1$^{-/-}$ and C57BL/6 mice were lethally irradiated and reconstituted with bone marrow from donor C57BL/6 or Ceacam1$^{-/-}$ mice. After 6 weeks, chimeras were injected s.c. with B16F10 melanoma cells and tumor growth in chimeras measured. Data represent mean ± SEM. *$0.01< P$ 0.05, **$0.001< P$ 0.01 (n=8 mice per group from two independent experiments). (**B**) Blood vessels in tumors were counted on frozen tissue after 17days. More than 8 fields of view were analyzed. Data represent mean ± SEM. ***P 0.001. (**C**) Immunohistochemisty staining of mouse B16 tumor tissue from chimeras with anti-CD31 antibody. Bar = 200µm. (**D**) B16 tumors were injected s.c. into

Ceacam1$^{-/-}$Rag1$^{-/-}$ and Rag1$^{-/-}$ and tumor growth was measured for 17 days. Data represent mean ± SEM. *0.01< P   0.05, **0.001<P   0.01 (n=10 mice per group from two independent experiments). (**E**) Blood vessels in tumors were counted on frozen tumor tissue collected from mice in (**D**) after 17days. Data represent mean ± SEM. ***P   0.001. (**F**) Immunohistochemisty staining of mouse B16 tumor tissue collected from mice in (**A**) after 17 days with anti-CD31. Bar = 200μm.
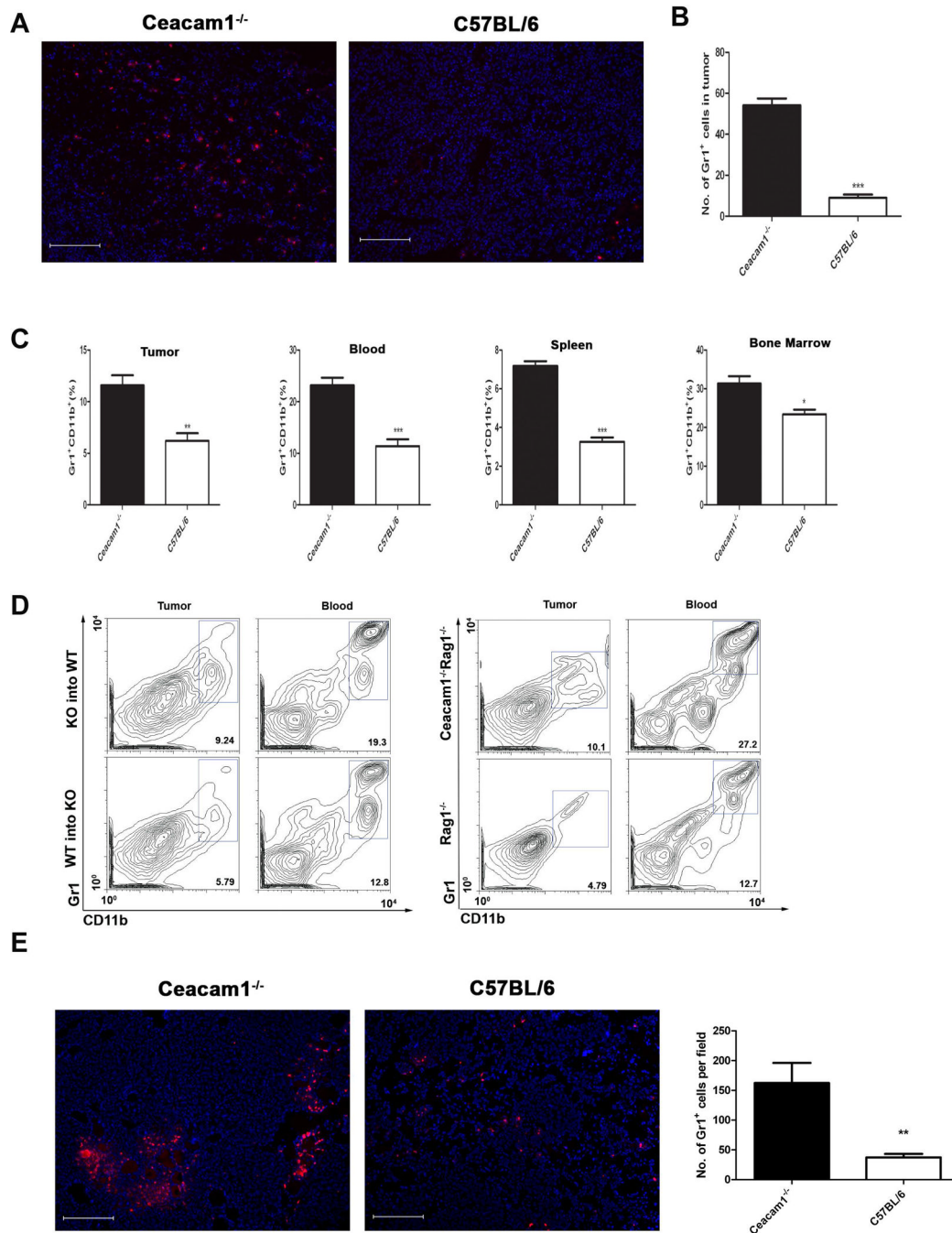
Figure 3. Infiltration of Gr1$^+$CD11b$^+$ myeloid cells is enhanced in tumors of Ceacam1$^{-/-}$ mice
(**A**) Immunofluorescent staining with Gr1$^+$ antibody (Red) plus DAPI (blue) of frozen tumor tissue harvested after 17 days. Bar = 200μm. (**B**) Quantitation of Gr1$^+$ cells in tumor was taken from immunofluoresecent staining in (**A**). More than 10 fields of view were analyzed. Data represent mean ± SEM. ***P 0.001. (**C**) Single-cell suspensions were prepared from B16 tumors harvested 17 days after tumor implantation. The mean percentage of Gr1$^+$CD11b$^+$ cells in tumor, blood, spleen and bone marrow from Ceacam1$^{-/-}$ and C57BL/6 tumor-bearing mice is shown in bar graphs. Data represent mean ± SEM, *0.01< P 0.05, **0.001<P 0.01, ***P 0.0001 (n=6 mice per group from three independent

experiments). (**D**) Representative flow cytometric analysis showing $Gr1^+CD11b^+$ myeloid population in chimeras tumor-bearing mice (left) and in $Ceacam1^{-/-}Rag1^{-/-}$ or $Rag1^{-/-}$ tumor bearing mice (right), (n=6 mice per group from three independent experiments). (**E**) Immunofluorescent staining with $Gr1^+$ antibody (Red) plus DAPI (blue) of frozen Matrigel plugs harvested after 6 days in CEACAM1−/− mice vs C57B/6 controls. Quantitation is shown to the right (**P<0.01). Bar = 200μm.
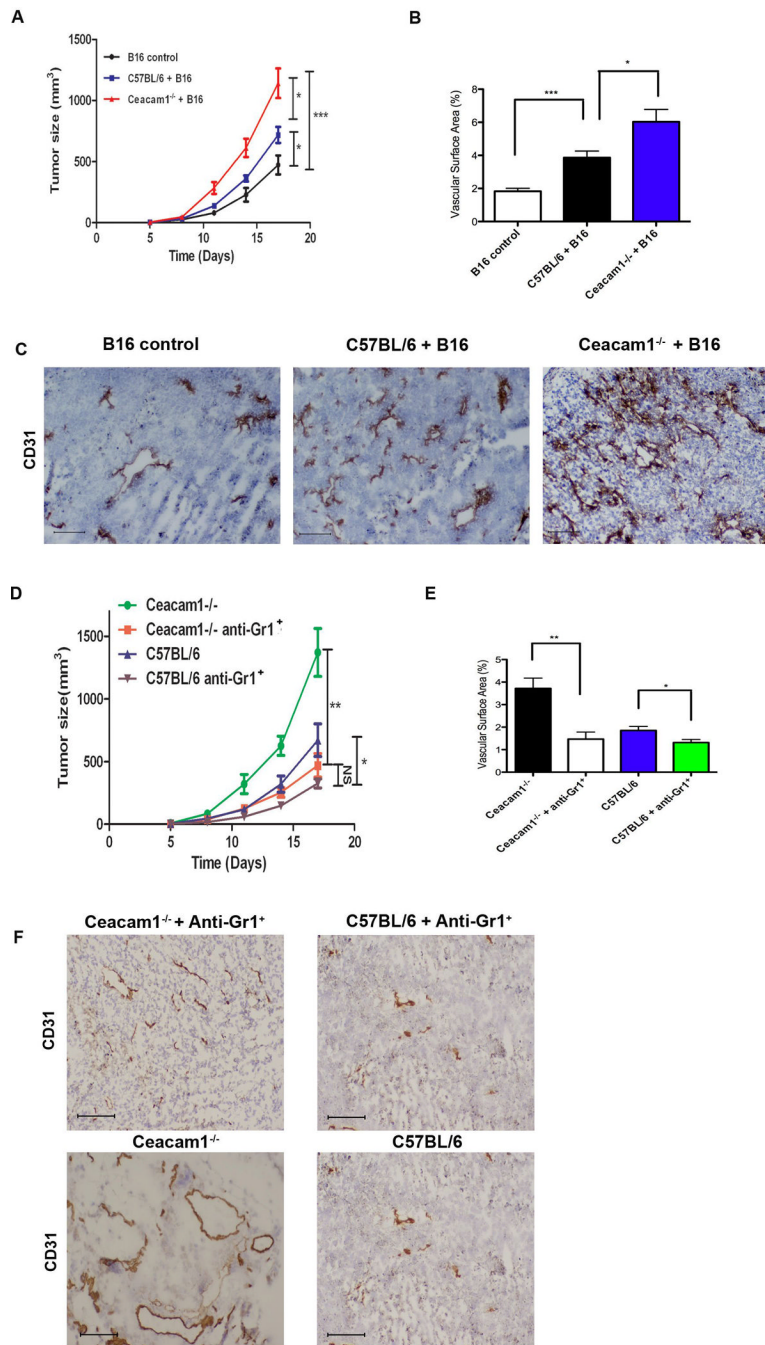
Figure 4. Gr1+CD11b+ myeloid cells are sufficient and necessary for enhanced tumor growth and angiogenesis in Ceacam1$^{-/-}$ mice

(**A**) Wild type mice injected s.c. with B16 tumor cells mixed with Gr1+CD11b+ cells enriched from tumor-bearing Ceacam1$^{-/-}$ mice (Ceacam1$^{-/-}$ +B16) or WT mice (C57BL/6+B16) or B16 alone (B16 control). Data represent mean ± SEM, *0.01< P   0.05, *** P   0.001 (n=6 mice per group from three independent experiments). (**B**) Blood vessels in tumors were counted from mice in (**A**) after 17 days. More than 8 fields of view were analyzed. Data represent mean ± SEM. **0.001< P   0.01, ***P   0.001. (**C**) Immunohistochemistry staining (anti-CD31 antibody) of mouse B16 tumor tissue collected from mice in (**A**) after 17 days. (**D**) Gr1+CD11b+ cells were depleted by anti-Gr1 Ab, and

compared to untreated animals. Data represent mean ± SEM. *0.01< P 0.05, **0.001< P 0.01, NS (no significance) (n=8 mice per group from two independent experiments). (**E**) Frozen tumor tissue harvested after 17 days were stained with anti-CD31 antibody. Data represent mean ± SEM. ***P 0.001. (**F**) Immunohistochemistry staining (anti-CD31) of mouse B16 tumor tissue collected from mice in (**D**) after 17 days of treatment with anti-CD31 antibody. Bar = 200μm.
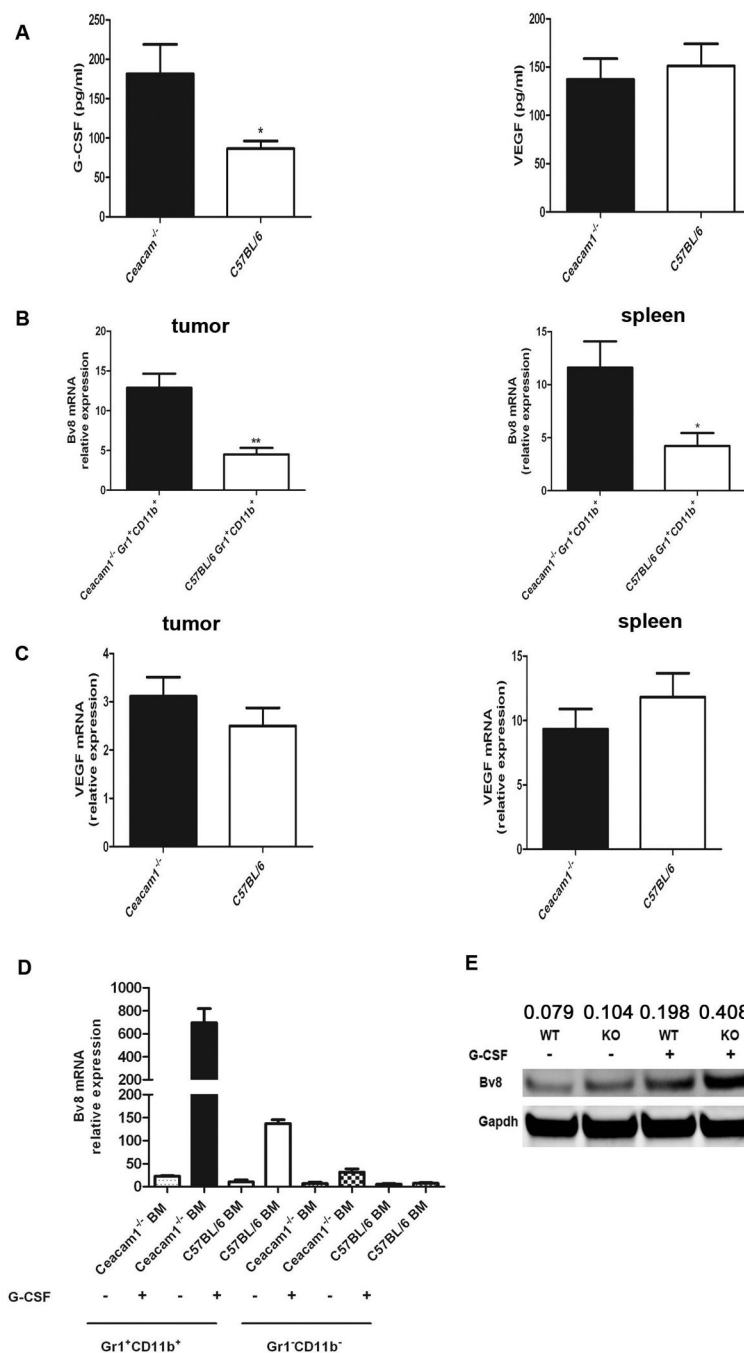
Figure 5. Bv8 is elevated in Ceacam1$^{-/-}$ Gr1$^+$CD11b$^+$ myeloid cells
(**A**) G-CSF and VEGF secretion from B16 tumors from Ceacam1$^{-/-}$ and C57BL/6 was assessed by ELISA after 12-h culture. Data represent mean ± SEM *0.01< P 0.05, (**B**) Real-time PCR analysis of Bv8 mRNA transcript levels in Gr1$^+$CD11b$^+$ cells enriched from spleen and tumor of Ceacam1$^{-/-}$ and C57BL/6 tumor-bearing mice. Data represent mean ± SEM *0.01< P 0.05, **0.001< P 0.01. (**C**) Real-time PCR analysis of VEGF mRNA transcript levels in Gr1$^+$CD11b$^+$ cells enriched from tumor and spleen of Ceacam1$^{-/-}$ and C57BL/6 tumor-bearing mice. Data represent mean ± SEM. (**D**) Bv8 mRNA levels are upregulated by G-CSF in Ceacam1$^{-/-}$ Gr1$^+$CD11b$^+$ cells. Real-time PCR showing Bv8

mRNA transcript levels in Gr1$^+$CD11b$^+$ or Gr1$^-$CD11b$^-$ cells enriched from Ceacam1$^{-/-}$ or C57BL/6 bone marrow, with or without G-CSF treatment (50 ng/ml). Data represent mean ± SEM. (**E**) Immunoblot analysis of Bv8 in Ceacam1$^{-/-}$ and C57BL/6 Gr1$^+$CD11b$^+$ cells with or without G-CSF treatment (50 ng/ml). Qunatitation by densitomtery and normalized to GAPDH.
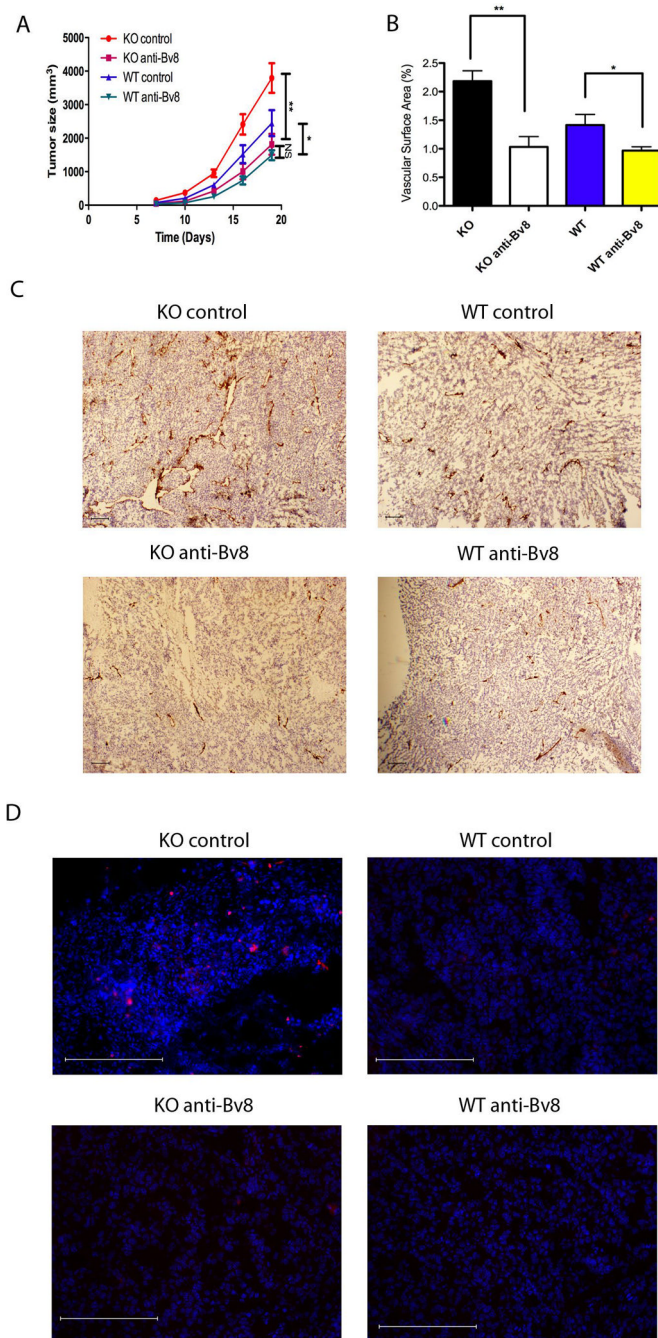
Figure 6. Tumor growth and angiogenesis are reduced in anti-Bv8 treated Ceacam1$^{-/-}$ mice
(**A**) Anti-Bv8 blocking antibody reduced tumor growth (n=6 mice per group) in Ceacam1$^{-/-}$ mice bearing B16 tumors. Data represent mean ± SEM. *0.01< P   0.05, **0.001< P   0.01. (**B**) Blood vessels in tumors were counted based on immunohistological analysis with anti-CD31 of frozen tumor tissue collected from mice in (**A**) after 17 days. More than 8 fields of view were analyzed. Data represent mean ± SEM. **0.001< P   0.01. (**C**) Immunohistochemistry staining of mouse tumor tissue collected from mice in (**A**) after 17 days with anti-CD31 antibody. Bar = 200μm. (**D**) Immunofluorescent staining of tumor associated Gr1^{+} cells. Bar = 200μm.
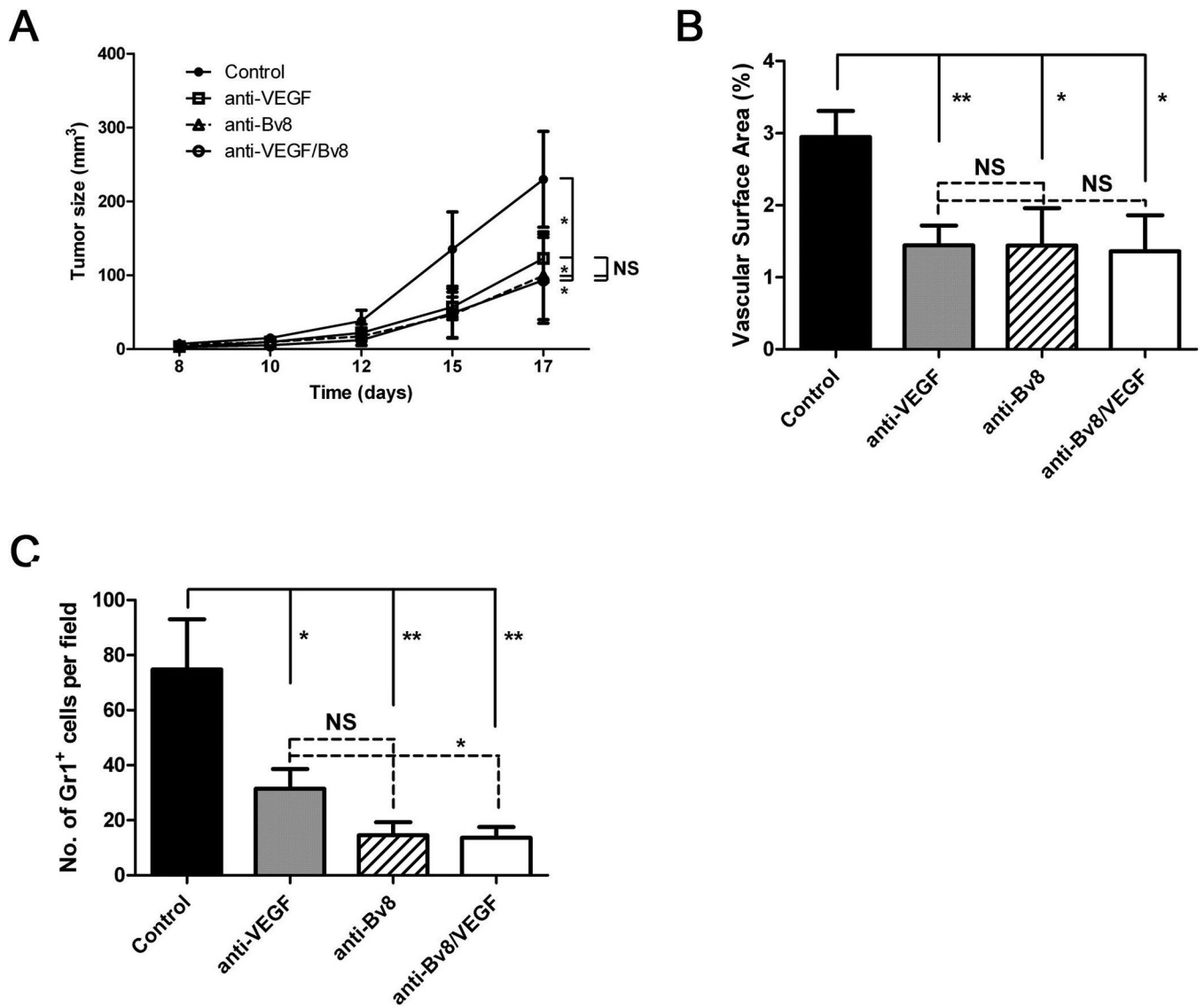
Figure 7. Tumor growth and angiogenesis are reduced in ant-VEGF or combined anti-VEGF anti-Bv8 treated Ceacam1$^{-/-}$ mice

(**A**) Anti-VEGF, anti-Bv8, or combined blocking antibodies reduced tumor growth (n=6 mice per group) in Ceacam1$^{-/-}$ mice bearing B16 tumors. Data represent mean ± SEM, *P 0.01. (**B**) Blood vessels in tumors were counted based on immunohistological analysis with anti-CD31 of frozen tumor tissue collected from mice in (**A**) after 17 days. More than 8 fields of view were analyzed. Data represent mean ± SEM. **0.001< P 0.01. (**C**) Immunofluorescent staining of tumor associated Gr1^{+} cells. Data represent mean ± SEM. **0.001< P 0.01.